Pergamon

Int. J. Heat Mass Transfer. Vol. 40, No. 3, pp. 737–744, 1997

0017–9310/97 $15.00+0.00

PII: S0017-9310(96)00092-0

TECHNICAL NOTES

Mixed binary convection in a rotating disk chemical vapor deposition reactor

W. S. WINTERS and G. H. EVANS
Sandia National Laboratories, Livermore, CA 94550, U.S.A.

and

R. GREIF
Mechanical Engineering Department, University of California, Berkeley, CA 94720, U.S.A.

(*Received* 20 *June* 1995 *and in final form* 29 *February* 1996)

INTRODUCTION

Gas mixing is an important aspect of transport in chemical vapor deposition (CVD) processes. In some cases undesirable reactions occur between unheated reactants, requiring the reacting gases to remain separated prior to reactor entry. Carrier gases tend to be light species such as H_2 and He although N_2 is sometimes used. Typically, reacting gases are much heavier species with molecular weights exceeding 100 g mole^{-1} for some species such as TMG and SiF_4. Large differences in temperature and/or molecular weight can result in significant buoyancy and unstable and recirculating flow.

The rotating disk reactor (RDR) is an attempt to take advantage of the uniform transport properties characteristic of an infinite rotating disk in an infinite medium. Parameters that can cause deviations from the ideal flow behavior include variable properties, reactor geometry, and gas flow rates. Previous studies by Evans and Greif [1, 2], Patnaik *et al.* [3] and Fotiadis *et al.* [4] have examined these effects for a single component gas in a nonisothermal RDR. Palmateer *et al.* [5] noted convective instabilities in an experimental study of isothermal gas mixing in a stagnation flow reactor; they found that convective cells were not eliminated when the susceptor was rotated between 10 and 1200 rpm. The present study examines the effects of gas mixing on flow behavior in a RDR. We restrict the study to an isothermal binary gas system flowing over a high speed rotating disk in a cylindrical reactor. Complex flow fields are produced as a result of the interactions that occur between the solutal buoyant force, the forced flow, and the flow induced by the rotation of the disk. Deviation from the ideal rotating disk flow is quantified with a radial shear stress parameter.

MODEL

A cylindrical reactor of radius $\bar{r}_0$ and height $\bar{H}$ contains a spinning disk of radius $\bar{r}_d$ located a distance $\bar{h}$ from the top inlet (cf. Fig. 1). The incoming flow is partitioned into two sections, a circular "core" of radius $\bar{r}_c$ and an annular "shroud" bounded by radii $\bar{r}_c$ and $\bar{r}_0$. In this study $\bar{r}_c = \bar{r}_d$, with uniform and equal core and shroud inlet velocities, $\bar{u}_{in}$. The core and shroud gases enter through the top, mix as they flow downward over the rotating disk, and exit through the annular channel at the bottom. When the core and shroud gas compositions are identical this situation reduces to the single species rotating disk problem (see e.g. [1–4]). Here we study the influence of nonuniform inlet composition on the behavior of isothermal flow in the reactor. Unless otherwise specified the shroud is H_2; the core gas is either NH_3 or a mixture of NH_3 and H_2.

The dimensionless cylindrical axisymmetric equations for mass, momentum and species conservation in a binary mixture with no gas phase or surface reactions are:

$$\frac{1}{r}\frac{\partial(r\rho v)}{\partial r}+\frac{\partial(\rho u)}{\partial x}=0 \tag{1}$$

$$\frac{1}{r}\frac{\partial}{\partial r}\left(r\rho vu-\frac{r\mu}{Re_\omega}\frac{\partial u}{\partial r}\right)+\frac{\partial}{\partial x}\left(\rho uu-\mu\frac{\partial u}{\partial x}\right)=$$

$$-\frac{\partial p_m}{\partial x}+\frac{Gr}{Re_\omega^{3/2}}\frac{(1-\rho)}{(1-\rho_s)}\left(\frac{\bar{r}_d}{\bar{h}}\right)^3+\frac{1}{r}\frac{\partial}{\partial r}\left(r\mu\frac{\partial v}{\partial x}\right)$$

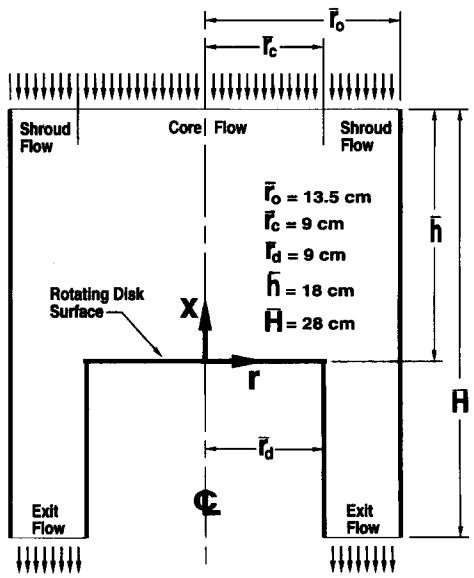

Fig. 1. Rotating disk reactor geometry.

NOMENCLATURE

$\mathscr{D}$ binary diffusion coefficient
$Gr/Re^{3/2}$ mixed convection parameter (MCP), $\bar{g}(\bar{\rho}_c-\bar{\rho}_s)/(\bar{\rho}_c\bar{v}_c^{1/2}\bar{\omega}^{3/2})(\bar{h}/\bar{r}_d)^3$
M_{mix}, M_k mixture and species k molecular weights
P pressure
Pe_{in} inlet Peclet number, $Pe_{in} = Re_{in}Sc = SP\sqrt{Re_\omega}$
Re_ω disk Reynolds number, $\bar{r}_d^2\bar{\omega}/\bar{v}_c$
Re_{in} inlet Reynolds number, $2\bar{r}_0\bar{u}_{in}/\bar{v}_c$
$Re_{in}/\sqrt{Re_\omega}$ flow parameter (SP), $2\bar{r}_0\bar{u}_{in}/(\bar{r}_d\sqrt{\bar{\omega}\bar{v}_c})$
Sc Schmidt number, $\bar{v}_c/\bar{\mathscr{D}}_c$
T temperature
X_k, Y_k mole and mass fraction of species k
f ratio w/r
h disk to inlet height
$\bar{h}$ dimensional disk to inlet height
$\bar{H}$ dimensional reactor height
p_m pressure in momentum equations
r radial coordinate
$\bar{r}_c$ dimensional core radius
$\bar{r}_d$ dimensional disk radius
$\bar{r}_0$ dimensional reactor radius
t time
u axial velocity component
v radial velocity component
w circumferential velocity component
x axial coordinate.

Greek symbols
ρ mixture density
ν mixture kinematic viscosity
μ mixture dynamic viscosity
ξ shear stress parameter, equation (8)
ω disk spin rate.

Subscripts and superscripts
d disk quantity
s inlet shroud (for $\bar{r}_d \leqslant \bar{r} \leqslant \bar{r}_0$, $\bar{x} = \bar{h}$)
c inlet core quantity (for $0 \leqslant \bar{r} \leqslant \bar{r}_d$, $\bar{x} = \bar{h}$)
$-$ dimensional quantity
in evaluated at reactor inlet.

$$+\frac{\partial}{\partial x}\left\{\mu\frac{\partial u}{\partial x}-\frac{2\mu}{3}\left[\frac{1}{r}\frac{\partial(rv)}{\partial r}+\frac{\partial u}{\partial x}\right]\right\} \quad (2)$$

$$\frac{1}{r}\frac{\partial}{\partial r}\left(r\rho vv-\frac{r\mu}{Re_\omega}\frac{\partial v}{\partial r}\right)+\frac{\partial}{\partial x}\left(\rho uv-\mu\frac{\partial v}{\partial x}\right)=$$

$$-\frac{1}{Re_\omega}\frac{\partial p_m}{\partial r}-r\rho f^2+\frac{1}{Re_\omega}\frac{1}{r}\frac{\partial}{\partial r}\left\{r\mu\left[\frac{\partial v}{\partial r}-\frac{2}{3}\left(\frac{1}{r}\frac{\partial(rv)}{\partial r}+\frac{\partial u}{\partial x}\right)\right]\right\}$$

$$-\frac{1}{Re_\omega}\frac{\mu}{r}\left\{\frac{2v}{r}-\frac{2}{3}\left[\frac{1}{r}\frac{\partial(rv)}{\partial r}+\frac{\partial u}{\partial x}\right]\right\}+\frac{1}{Re_\omega}\frac{\partial}{\partial x}\left(\mu\frac{\partial u}{\partial r}\right) \quad (3)$$

$$\frac{1}{r}\frac{\partial}{\partial r}\left(r\rho vf-\frac{r\mu}{Re_\omega}\frac{\partial f}{\partial r}\right)+\frac{\partial}{\partial x}\left(\rho uf-\mu\frac{\partial f}{\partial x}\right)=$$

$$-\frac{2\rho vf}{r}+\frac{1}{Re_\omega}\frac{2\mu}{r}\frac{\partial f}{\partial r} \quad (4)$$

$$\frac{1}{r}\frac{\partial}{\partial r}\left(r\rho vY_k-\frac{r\rho\mathscr{D}}{Re_\omega\cdot Sc}\frac{\partial Y_k}{\partial r}\right)+\frac{\partial}{\partial x}\left(\rho uY_k-\frac{\rho\mathscr{D}}{Sc}\frac{\partial Y_k}{\partial x}\right)=0 \quad (5)$$

where $f = w/r$; u, v, w are the dimensionless axial, radial, and circumferential velocity components, respectively. The parameters are: $Gr = \bar{g}(\bar{\rho}_c-\bar{\rho}_s)\bar{h}^3/(\bar{\rho}_c\bar{v}_c^2)$, $Re_\omega = \bar{r}_d^2\bar{\omega}/\bar{v}_c$ and $Sc = \bar{v}_c/\bar{\mathscr{D}}_c$ ($\bar{\omega}$ is the disk spin rate; $\bar{v}$ is the mixture kinematic viscosity; $\mathscr{D}$ is the binary diffusion coefficient); the mixture density ρ and viscosity μ are normalized based on the reactor inlet mixture composition in the core region (subscript c). The usual scaling (Evans and Greif [1]; White [6]) for a rotating disk has been used: $\sqrt{\bar{\omega}\bar{v}_c}$ for the axial component of velocity, $\bar{r}_d\bar{\omega}$ for the radial and circumferential components of velocity, $\sqrt{\bar{v}_c/\bar{\omega}}$ for the axial coordinate, and $\bar{r}_d$ for the radial coordinate, where symbols with overbars represent dimensional quantities. The boundary conditions are:

$$\{x = 0, 0 \leqslant r \leqslant 1\}: \quad u = v = \partial Y_k/\partial x = 0, \quad f = 1;$$

$$\{x = h, 0 \leqslant r \leqslant 1\}: \quad X_k = X_{kc}, k = H_2, NH_3$$

$$\{x = h, 1 \leqslant r \leqslant \bar{r}_0/\bar{r}_d\}: \quad X_k = X_{ks}, k = H_2, NH_3;$$

$$\{r = \bar{r}_0/\bar{r}_d, h-H \leqslant x \leqslant h\}: \quad u = v = f = \partial Y_k/\partial r = 0$$

$$\{x = h, 0 \leqslant r \leqslant \bar{r}_0/\bar{r}_d\}:$$

$$v = f = 0, u = Re_{in}/\sqrt{Re_\omega}\cdot[\bar{r}_d/(2\bar{r}_0)]$$

$$\{r = 0, 0 \leqslant x \leqslant h\}:$$

$$\partial u/\partial r = \partial f/\partial r = \partial Y_k/\partial r = v = 0;$$

$$\{r = 1, h-H \leqslant x \leqslant 0\}: \quad u = v = f = \partial Y_k/\partial r = 0$$

where $Re_{in} = 2\bar{r}_0\bar{u}_{in}/\bar{v}_c$, $X_k = Y_k\bar{M}_{mix}/\bar{M}_k$ and X_k, Y_k, $\bar{M}_k$, $\bar{M}_{mix}$ are species k mole and mass fractions, molecular weight, and mixture molecular weight, respectively. Fully developed conditions are applied at the outflow boundary.

The equations are integrated over control volumes and discretized using the hybrid differencing scheme (Patankar [7]). The SIMPLER method is used to determine the pressure, p_m. A sequential interative line relaxation scheme is used to solve the equations. Equation (5) is solved for H_2; the NH_3 mass fraction being determined by $(1 - Y_{H2})$.

Underrelaxation factors (0.3–0.7) were used for the momentum and species mass conservation equations; no underrelaxation was applied to the pressure equation. Iterations were continued (typically 5000 to 15 000) until changes in the radial component of shear stress at the disk surface (the most sensitive quantity) were negligible.

The results presented here were obtained on a nonuniform grid of 100×65 control volumes in the x and r directions, respectively, with finer grid spacings near the disk ($x = 0$) and the symmetry axis ($r = 0$). Calculations were also made on a nonuniform x, r grid of 80×55 control volumes. Results

for the radial component of the shear stress differed by less than 5% for the two grid distributions. The fine grid resolution of the disk boundary layer was adequate since calculations differed from the similarity solution for the flow over an infinite rotating disk by less than 1%.

RESULTS AND DISCUSSION

A well-known characteristic for isothermal single species flow over an infinite rotating disk is the uniformity of the resulting boundary layers (see e.g. [6]). This leads to:

$$\frac{\bar{\tau}_{drx}}{\bar{r}} = \frac{\bar{\mu}}{\bar{r}} \left.\frac{\partial \bar{v}}{\partial \bar{x}}\right|_{\bar{x}=0} = \text{constant for all } \bar{r} \tag{6}$$

where $\bar{\tau}_{drx}$ is the radial component of the shear stress evaluated at the disk surface. In an actual reactor, uniformity of the shear stress parameters, $\bar{\tau}_{drx}/\bar{r}$, is a measure of how well the flow simulates the ideal infinite rotating disk flow. Flow uniformity is an important reactor design goal since it is often a necessary condition for deposition uniformity. The influence of nonuniform inlet composition on reactor flow quality is determined by comparing dimensionless shear stress parameter profiles over the disk (plots of ξ vs r); the normalization factor is

$$\left.\frac{\bar{\tau}_{drx}}{\bar{r}}\right|_{1D} = 0.51023 \sqrt{\bar{\rho}_{NH_3} \bar{\mu}_{NH_3} \bar{\omega}^3}. \tag{7}$$

Equation (7) is the shear stress parameter for NH_3 flowing over an infinite rotating disk [6]. Hence,

$$\xi = \frac{\bar{\tau}_{drx}/\bar{r}}{(\bar{\tau}_{drx}/\bar{r})_{1D}} = \frac{(\bar{\mu}/\bar{r})(\partial \bar{v}/\partial \bar{x})_{\bar{x}=0}}{0.51023 \sqrt{\bar{\rho}_{NH_3} \bar{\mu}_{NH_3} \bar{\omega}^3}}. \tag{8}$$

Figures 2 and 3 show the effects of pressure and temperature on the flow and mixing in the RDR for a disk rotation rate of 500 rpm for core and shroud gases NH_3 and H_2 respectively. The inlet velocity, $\bar{u}_{in}$, was uniform and equal to the infinite rotating disk velocity V^* (White [6]) for properties of NH_3 ($\bar{u}_{in} = V^* = -0.884\sqrt{\bar{\omega}\bar{\nu}_c}$). We define a "starving parameter" $SP = Re_{in}/\sqrt{Re_\omega}$, where Re_{in} is the inlet Reynolds number, and Re_ω is the spin Reynolds number. Substituting V^* for $\bar{u}_{in}$ in Re_{in} yields $SP = 1.768\bar{r}_0/\bar{r}_d = 2.65$. For $\bar{u}_{in} < V^*$ the flow is "starved" (i.e. the core flow rate is less than the induced flow rate for the infinite rotating disk). For a single species with thermal buoyancy, starving the rector can lead to unstable flows [1].

The radial distribution of ξ is shown in Fig. 2(a) for five cases A–E. Case E is a benchmark calculation (76 torr and 523 K) performed with NH_3 in both the core and the shroud. Except near the outer edges of the disk (not shown) the solution was in agreement with the infinite rotating disk similarity solution.

Case A is identical to Case E except that H_2 is substituted for the NH_3 in the shroud. Introduction of H_2 creates a potential for buoyancy in the flow which can be characterized by a mixed convection parameter, MCP:

$$MCP = \frac{Gr}{Re_\omega^{3/2}} = \frac{\bar{g}(\bar{\rho}_c - \bar{\rho}_s)}{(\bar{\rho}_c \bar{\nu}^{1/2} \bar{\omega}^{3/2})} \left(\frac{\bar{h}}{\bar{r}_d}\right)^3. \tag{9}$$

Introducing H_2 into the shroud (Case A) increases the MCP from 0.0 to 8.4 resulting in a non-uniform distribution of ξ and a considerable departure from ideal single species flow. Increasing the temperature to 800 K (Case B) results in a lowering of ξ. Reducing the pressure to 50 torr (Case C) and 25 torr (Case D) causes further reductions in ξ. Uniformity is improved with decreasing pressure and increasing temperature. We note that both MCP and Re_ω decreased from Cases A to D. Figure 2(b) shows the radial variation of the concentration of NH_3 one centimeter above the disk. With decreasing MCP, the decreased concentration of NH_3 is due to increased mixing with H_2.

The nature of the idealized flow departure for Cases A–D is seen in Fig. 3. Reactor crossections show computed streamlines superimposed on color-filled contours of NH_3 concentration. High concentrations of NH_3 are shown in red while high concentrations of H_2 are shown in dark blue. When the flow exits the reactor the two gases are completely mixed (blue–green). A strong recirculation in Case A results in high shear stresses shown near the centerline on Fig. 2(a). Increasing the temperature (Case B) and decreasing the pressure (Cases C and D) reduce the size and strength of the recirculation resulting in more radial mixing of NH_3 and H_2 and more uniform stress distributions. The range of streamlines plotted for Case C does not show the small weak recirculation which existed near the wall. Case D is completely free of the recirculation and resembles the ideal single component flow expected (and verified) from Case E. The general lowering in shear stress levels from Cases A to D is primarily the result of increased mixing in the core region above the disk. Note the lower reactor centerline NH_3 concentration profiles plotted in Fig. 2(c); the Peclet number for mass transfer based on the inlet flow, $Pe_{in} = Re_{in}Sc = SP\sqrt{Re_\omega}$, decreases from 17 for Case A to 7 for Case D. Mixing reduces the molecular weight of the gas below that of pure NH_3 leading to lower shear stress levels. An additional reason for lowered stress levels near the centerline is reduced buoyancy.

Figure 4(a) illustrates the effect of varying the core inlet composition for fixed conditions of 76 torr, 523 K and 100 rpm. The solid lines show ξ profiles for cases in which the inlet velocity equals the ideal value for the specified NH_3–H_2 core mixture. Hence, each solid curve is the result of a calculation made with the inlet velocity $\bar{u}(\bar{r},\bar{h}) = V^*$ for core compositions of 100, 75, 50 and 25% NH_3. Dashed lines show ξ profiles for cases in which inlet velocity is maintained at a constant value for core compositions of 75, 50 and 25% NH_3. The constant value is the ideal velocity for 100% NH_3, i.e. $\bar{u}(\bar{r},\bar{h}) = -6.16\ \text{cm s}^{-1}$. Since introducing H_2 into the core inlet increases V^*, the dashed lines represent, shear profiles for flows which are starved with respect to the inlet core composition. The variations in inlet velocity and core composition give rise to the range of values of MCP, Re_ω and SP shown adjacent to each curve.

Lowering the NH_3 core composition results in lowered values of MCP and a corresponding improvement in shear stress uniformity; the magnitude of the shear stress is also lowered. Similar results for 500 rpm are shown in Fig. 4(b). The increased rotation rate results in larger values of Re_ω and correspondingly lower values in MCP. Lowering the MCP has the expected result of improving shear stress uniformity. Overall shear stress levels are lowered indicating a decrease in the strength and size of the flow recirculation that accompanies lower values in MCP and the decreasing NH_3 concentration.

In all cases shown in Fig. 4, starving the flow results in improved uniformity. This is in direct contrast to starved single species flow in the presence of thermal buoyancy which usually results in degraded uniformity [1]. In the isothermal two-species flows shown here, starving the flow causes diffusion to overcome convection and become the dominant mechanism for mass transport, resulting in enhanced mixing. For example, for the two 25% NH_3 cases shown in Fig. 4(a), the inlet Peclet numbers ($Re_{in}Sc$) are 12.5 for the unstarved flow and 7.5 for the starved flow.

The effect of starving or over-supplying a reactor having pure NH_3 in the core and H_2 in the shroud at the inlet is illustrated in Fig. 5. Distributions of ξ for 100 rpm, 76 torr, 523 K ($Re_\omega = 183$, MCP = 94) are shown for inlet velocities ranging from 0.2 cm s^{-1} (SP = 0.09) to 45 cm s^{-1} (SP = 19). As previously noted starving the two species flow actually improves shear stress uniformity. The uniformity improvements occur in spite of the fact that the flow recirculation

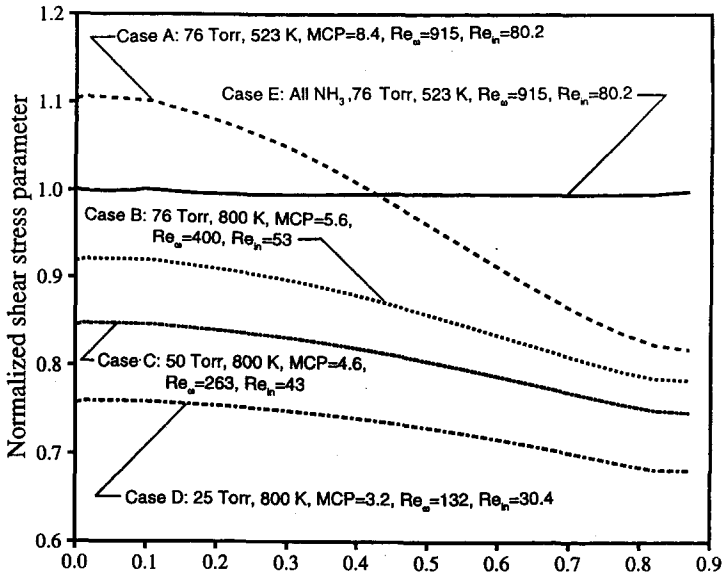

(a) Normalized shear stress at disk surface.

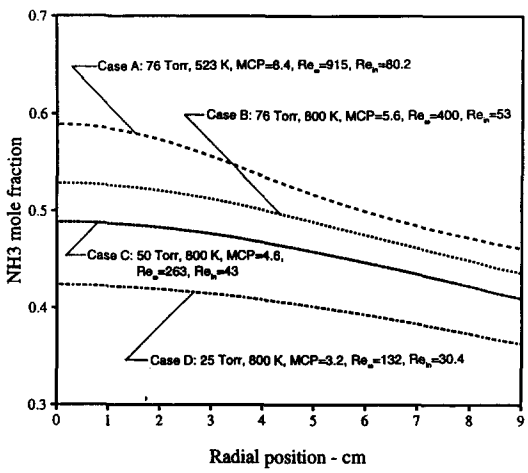

(b) Ammonia radial concentration profiles 1.0 cm above the disk surface.

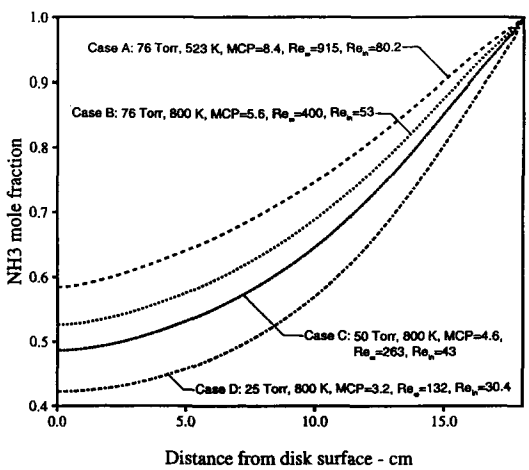

(c) Ammonia concentration profiles along the reactor centerline.

Fig. 2. Influence of pressure and temperature for 500 rpm, SP = 2.65. Cases A–D have NH_3 in core inlet and H_2 in shroud inlet. Case E has NH_3 in core and shroud inlets.

persists even for inlet velocities as small as 0.2 cm s^{-1}. For values of SP greater than 2.65, the rotating disk is over-supplied. Eventually at the highest flow condition (SP = 19), the forced flow overcomes the effects of buoyancy and recirculations disappear.

CONCLUSIONS

Introducing two separated gas species at the inlet of a rotating disk reactor can result in flow instabilities similar to those observed in single species flow with thermal buoyancy. The strength of the flow recirculation and the resulting departure from ideal flow can be characterized using a convection parameter based on the density difference of the incoming streams. Higher pressures, lower temperatures, and larger inlet density differences lead to larger mixed convection parameters and more unstable flow. Lowering the inlet velocity level (even starving the disk) leads to a more uniform boundary layer on the rotating disk and enhanced mixing at the disk surface. However, a large flow recirculation persists outside the boundary layer. Significantly over-supplying the rotating disk overcomes the effect of buoyancy and eliminates the recirculation.

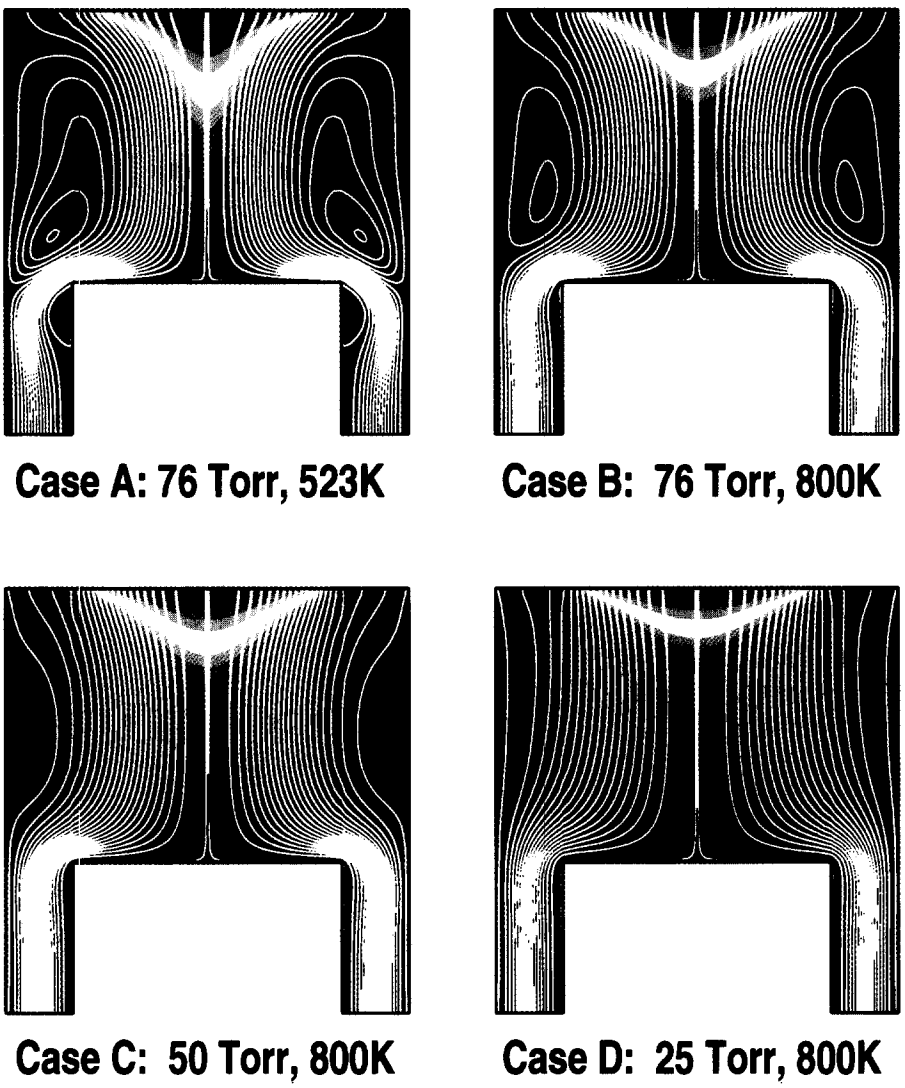

Fig. 3. Color filled contours of NH_3 concentration (red = high, blue = low) with superimposed streamlines.

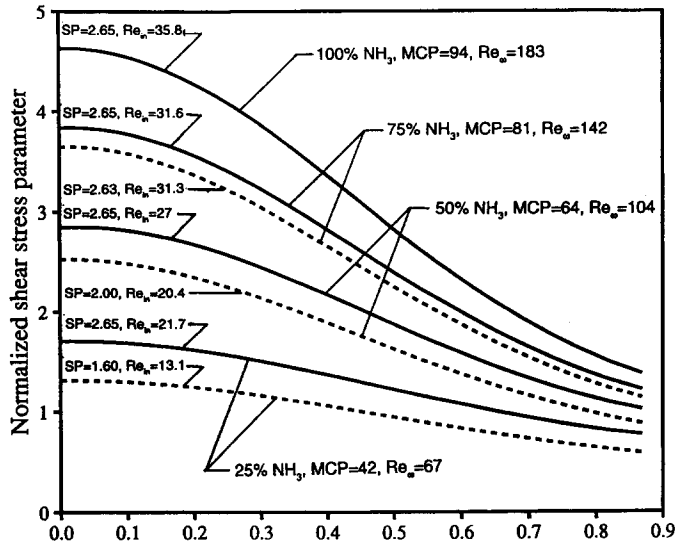

(a) Disk spin rate 100 RPM.

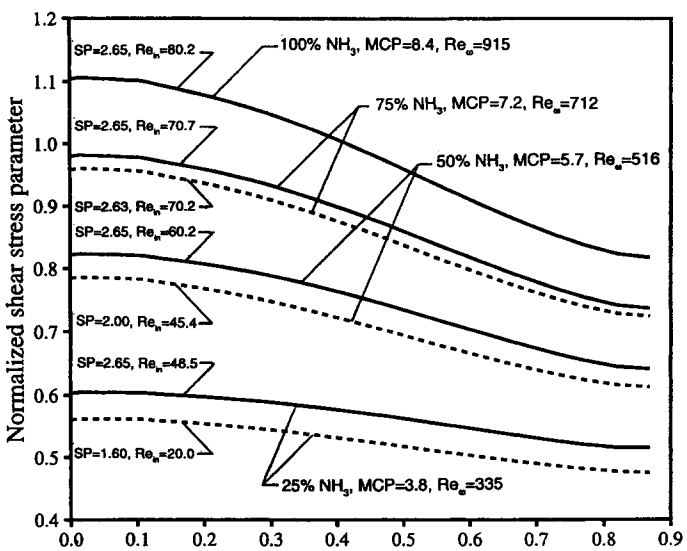

(b) Disk spin rate 500 RPM.

Fig. 4. Influence of varying core composition for 76 torr, 523 K. Core inlet is shown on plots. Shroud inlet is H_2.

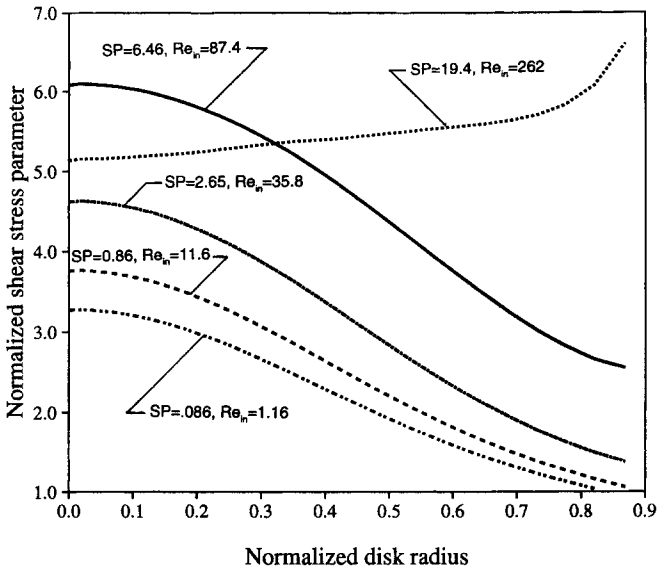

Fig. 5. Influence of starving/over-supplying rotating disk flow for 100 rpm, 76 torr, 523 K, NH_3 core inlet, H_2 shroud inlet, MCP = 94, Re_ω = 183.

Acknowledgements—The authors would like to thank Rick Stall of Emcore Corporation for many valuable discussions and information during the course of this study. This work was supported by the U.S. Department of Energy.

REFERENCES

1. G. Evans and R. Greif, A numerical model of the flow and heat transfer in a rotating disk chemical vapor deposition reactor, *J. Heat Transfer* **109,** 928–935 (1987).
2. G. Evans and R. Greif, Effects of boundary conditions on the flow and heat transfer in a rotating disk chemical vapor deposition reactor, *Numer. Heat Transfer* **12,** 243–252 (1987).
3. S. Patnaik, R. A. Brown and C. A. Wang, Hydrodynamic dispersion in rotating disk OMVPE reactors: numerical simulation and experimental measurements, *J. Crystal Growth* **96,** 153–174 (1989).
4. D. Fotiadis, S. Kieda and K. Jensen, Transport phenomena in vertical reactors for metalorganic vapor phase epitaxy—I. Effects of heat transfer characteristics, reactor geometry, and operating conditions, *J. Crystal Growth* **102,** 441–470 (1990).
5. S. C. Palmateer, S. H. Groves, C. A. Wang, D. W. Weyburne and R. A. Brown, Use of flow visualization and tracer gas studies for designing an InP/InGaAsP OMVPE reactor, *J. Crystal Growth* **83,** 202–210 (1987).
6. F. M. White, *Viscous Fluid Flow*. McGraw-Hill, New York (1974).
7. S. V. Patankar, *Numerical Heat Transfer and Fluid Flow*. McGraw-Hill, New York (1980).